

Contents

- 1 Introduction
- 2 Objectives
- 2 Study methods
- 3 Test flight details
- 4 Results and discussion
- 10 Conclusions
- 10 References
- 11 Acknowledgements

Capabilities of airborne infrared remote sensing systems to detect hotspots

Abstract

The Forest Engineering Research Institute of Canada (FERIC) conducted a study to assess the reliability, effectiveness, and cost of airborne infrared remote sensing, mapping, and analysis systems used in Alberta. Field trials were conducted to develop assessment methods and to facilitate preliminary tests of the hotspot detection capabilities of two airborne infrared remote sensing systems: an AWIS (Airborne Wildfire Intelligence System) mounted on a twin-engine aircraft, and a FLIR 2000 mounted on a “birddog” aircraft. Logistic regression was used to develop probability of detection models for each of the sensor and aircraft platforms evaluated. This report also describes the development of a simple model that allows fire managers to assess the cost effectiveness of alternative technologies.

Keywords

Infrared, Fire control, Fire detection, AWIS, FLIR, Remote sensing, Sensors, Thermography.

Author

Judi Beck,
Protection Branch,
B.C. Ministry of Forests.
Formerly with FERIC's
Wildland Fire Operations
Research Group.

Introduction

Knowledge of the fire behaviour characteristics at various locations along the fire perimeter is vital to the safe and efficient deployment of fire suppression resources, but wildfire detection and mapping can be difficult when smoke, haze, and darkness reduce visibility. The infrared (IR) energy radiated by a fire penetrates smoke, darkness, and most haze, and this allows an infrared detector to locate fires that would otherwise be obscured. Alberta Sustainable Research Development's (SRD) Forest Protection Division asked FERIC to assess the detection capabilities and limitations of two airborne infrared remote sensing systems: an AWIS (Airborne Wildfire Intelligence System)¹ mounted on a twin-engine aircraft, and a FLIR 2000² mounted on SRD's “birddog” aircraft.

In Alberta, helicopters and fixed-wing aircraft have been used to carry infrared sensors

(Niederleitner 1976; Ogilvie and Young 1989). Airborne infrared remote sensing has been used to support many fire management activities such as fire detection, large fire reconnaissance, fire perimeter mapping, hotspot detection, and identification of weak points and breaks in fire control lines (Aldrich 1979; Billings 1986; Matthews 1997; Campbell et al. 2002). Handheld infrared systems, such as several AGA³ models, have been used from a helicopter at low altitude (less than 500 feet above ground level) to confirm that logging residue piles burned in the spring are fully extinguished. Helicopter infrared scanning missions have also been

¹ AWIS and the Airborne Wildfire Intelligence System are trademarks of Range and Bearing Environmental Resource Mapping Corporation, Pender Island, B.C.

² FLIR 2000 is a trademark of FLIR Systems, Inc., Portland, Ore.

³ AGA is a trademark of FLIR Systems, Inc., Portland, Ore.

applied to confirm that mop-up operations on large fires have completely extinguished all hotspots.

In 1991, the first gimballed forward-looking infrared unit (FLIR 2000) was mounted on a birddog aircraft, which is used in Alberta to lead an air attack group. The birddog carries an air attack officer who directs all airtanker (water bomber) operations and employs the infrared sensor technology to detect gaps or weak points in the fire retardant line that is laid by airtankers along the fire perimeter. Because of the potential to increase the cost effectiveness of airtanker operations (Woodard et al. 1993), Alberta's entire fleet of birddog aircraft was equipped with FLIR sensors in 1995. These units have also been used for missions to scan spring-burned piles and to support hotspot detection on large fires. The birddog-mounted FLIR (BD FLIR) is combined with a printer and a VHS recorder. Tapes for each mission are kept for evaluation and printed images can be dropped to ground crews, although the primary function of the birddog is to support airtanker operations rather than incident mapping. Moreover, the application of the imaged information is limited in the absence of a trained thermographer or infrared interpreter.

In 1999, the AWIS unit became operational. AWIS acquires digital thermal infrared images and records of inertia using a twin-engine aircraft that is IFR (Instrument Flight Rules) capable, although most scanning is conducted under VFR (Visual Flight Rules) conditions. Proprietary processing software is applied to perform geometric corrections and produce geo-referenced thermal image mosaics, which are then distributed via the Internet.

FERIC's study of the AWIS and BD FLIR is part of a larger research project to develop methods to evaluate and quantify the reliability, effectiveness, and cost of various airborne infrared remote sensing systems used in wildfire suppression operations in Alberta.

Objectives

The objectives of this study were to:

- Develop assessment methods and make preliminary quantitative tests of the detection capabilities of AWIS and BD FLIR infrared remote sensing systems.
- Develop a model that would allow fire managers to evaluate the detection capabilities of various airborne infrared remote sensing systems.
- Develop a model that would allow fire managers to assess the cost effectiveness of alternative technologies.

Study methods

Experimental fieldwork was carried out near Coalspur, 52 km south of Hinton, Alberta. A coal seam fire is permanently active within the study area. Artificial heat sources were also set up in an adjacent area, in the open and beneath a canopy of mature pine, to provide targets of known temperature and size. Litter and surface fuels in the open area were very sparse, and the forest understorey was comprised largely of moss.

Target sizes and temperatures were varied to determine how these parameters affect the detection capabilities of a given sensor. Target temperatures were designed to reach those typical of the various combustion phases of forest fuels, with temperatures of about 370, 590, and 860°C for smouldering, glowing, and flaming combustion, respectively. Camp

Forest Engineering Research Institute of Canada (FERIC)

Eastern Division and Head Office
580 boul. St-Jean
Pointe-Claire, QC, H9R 3J9

☎ (514) 694-1140
☎ (514) 694-4351
✉ admin@mtl.feric.ca

Western Division
2601 East Mall
Vancouver, BC, V6T 1Z4

☎ (604) 228-1555
☎ (604) 228-0999
✉ admin@vcr.feric.ca

Disclaimer

Advantage is published solely to disseminate information to FERIC's members and partners. It is not intended as an endorsement or approval of any product or service to the exclusion of others that may be suitable.

© Copyright 2004. Printed in Canada on recycled paper.



fuel, propane, and small sterno stoves produced targets of 150–250, 300–350, and 400–750°C, respectively. The sterno stove yields a very small (5.2 cm in diameter) but hot, open-flame target. Subtler but larger hotspots typical of smouldering and glowing combustion were emulated using camp fuel and propane stoves. To produce a uniform heat source of known size, a round plate of cast iron was placed on top of the camp fuel (26.5 or 30 cm in diameter) and propane (20 cm in diameter) stoves. Thermocouples and dataloggers were used to monitor target temperatures at one-second intervals for the duration of the test flight.

The targets were randomly distributed throughout the study area. The study area was approximately 220 × 100 m, and was designed so that it could be detected within a single image at the lowest flight altitude (approximately 2000 feet above ground level). This would result in a minimum of two infrared image pixels (approximately 20 m) between targets. The latitude and longitude of each target were recorded using a handheld GPS unit.

Smoke bombs were lit to obscure the general study area and to serve as a general navigational aid for the aircraft. Air temperature and relative humidity were measured periodically on the ground throughout the flight trials.

Test flight details

Test flights were carried out in August 2001 in the early morning at approximately 05:00 DST, and in the late afternoon at approximately 17:15. Weather conditions were calm and clear, but light cloud was encountered at about 8000 feet during the morning AWIS test flight. Image acquisition for all altitudes sampled took place over approximately one hour.

The detection performance of both AWIS and BD FLIR was worse in the afternoon than in the early morning, which confirmed that infrared detection flights should take place in the early morning. Therefore, the field trial results reflect the morning test flights only, when optimum conditions for infrared scanning existed.

Sensor performance was evaluated at altitudes of 2000 to 6000 feet. Although AWIS is used for scanning at higher altitudes, cloud cover precluded tests above 6000 feet on the morning of the field trial. A summary of the key mission details is given in Table 1.

Figures 1 and 2 are typical images produced by the AWIS and BD FLIR systems for these detection missions. Note that results for the BD FLIR system are available immediately upon aircraft landing. However, AWIS data must be processed before analytical results are made available, and image-processing time increases with the area scanned.

Table 1. Salient mission details for AWIS and FLIR infrared remote sensing field trials

Infrared system	Flight time	Mission altitude (ft./m)	Air temperature (°C)	Relative humidity (%)	Assumed emissivity ^a	Ground pixel area ^b (cm ²)
AWIS	05:03–5:51	3000/915	6.0	76	0.92	2 116
		4000/1220	6.4	71	0.92	3 844
		6000/1830	6.4	71	0.92	8 464
BD FLIR	07:23–08:14	2000/610	2.2	77	n.a.	7 410
		4000/1220	2.2	77	n.a.	29 641
		6000/1830	2.2	77	n.a.	66 692

^a Emissivity is the ratio of the radiation emitted by a surface to that emitted by a black body at the same temperature.

^b Ground pixel area is a measure of the area viewed by a single cell within a detector array of a sensor on a scanning system at a given altitude in a given instant in time.

Figure 1. Morning thermal image and hotspots identified by AWIS at 3000 feet AGL. The final product includes colour mapping details, not reproduced here, that highlight features such as roads, rivers, and elevation contours.

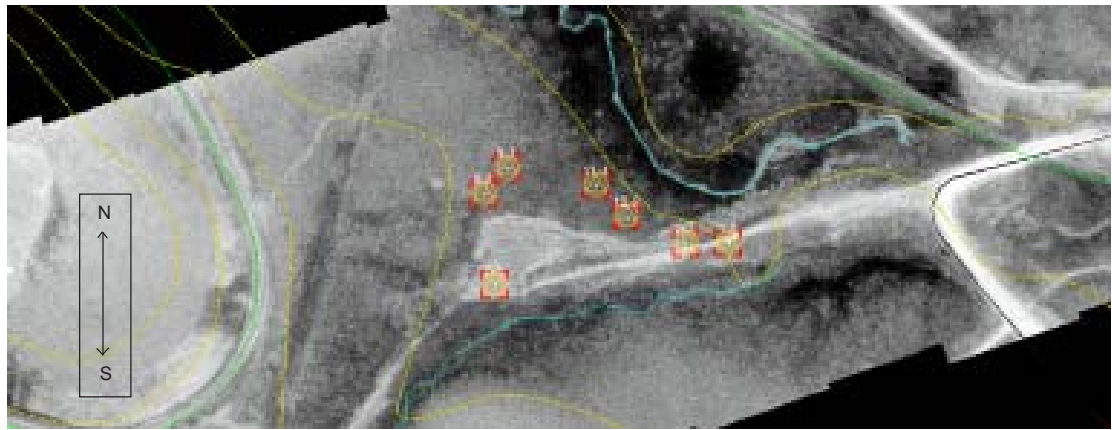
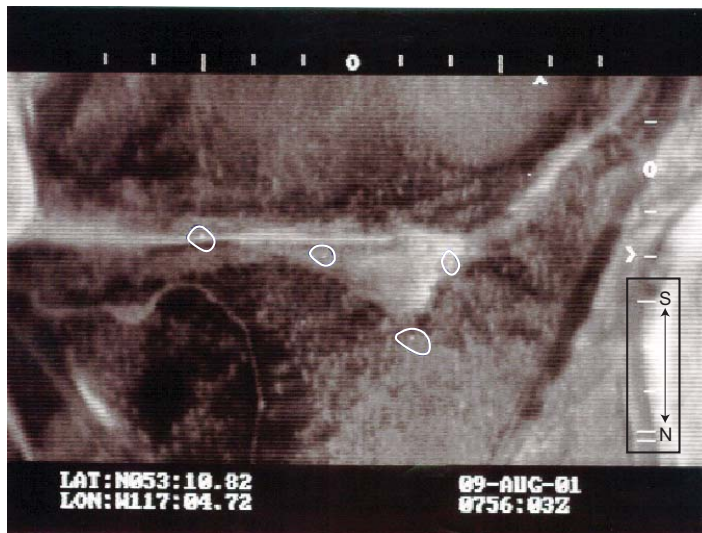


Figure 2. Morning thermal image and hotspots identified by BD FLIR at 4000 feet AGL.



thermocouple data indicated that the temperature of a target was not significantly higher than ambient, targets were classified as “Undetectable”.

The methods of target detection for these trials were typical of those for operational hotspot detection using AWIS and BD FLIR. To identify targets, AWIS processes radiometric values automatically, while local contextual visual assessment is used to control the quality of the automated

classification. Data processing is applied to detect hotspots automatically when a target’s radiometric value registers above a specified threshold for the mosaic scene (classified by a “Threshold” detection status). Other targets are identified using visual interpretation to determine when radiometric or image values exceed background values in the local vicinity (classified by “Background” detection status). Therefore, a Threshold or Background detection status indicates that the sensor was successful in detecting a target. AWIS applies other digital geographic information to confirm hotspots contextually, to minimize the number of false targets identified. The BD FLIR only allows visual interpretation of targets equivalent to the “Background” detection status of AWIS.

At all three test altitudes, both AWIS and BD FLIR identified a large hotspot at the location of the active coal seam fire. The very

Results and discussion

Field trial results

Eleven targets were established on the ground for the morning AWIS flight trials, and twelve were established for the BD FLIR. The size and temperature of each are given at the time of imaging (Tables 2 and 3). The detection status of each target indicates whether or not it was successfully detected. The thermocouples and dataloggers failed to record target temperatures at target sites 1, 11, and 13 for the AWIS flight trials and at site 3 for the BD FLIR flight trials. In the case of datalogger failures, those targets not detected have been classified with an “Unknown” detection status because it could not be confirmed that target temperatures were above ambient. Where a stove was not turned on or ran out of fuel, and the

Table 2. Size and temperature of each target as reported at the time of imaging by AWIS

Mission altitude (feet)	Target identifier ^a	Target exposure	Time of sample	Target diameter (cm)	Target area (cm ²)	Target to pixel area ratio (%)	Actual target temperature (°C)	Imaged target temperature (°C)	Detection status	
3000	1	Open	5:46:22	20.0	314.2	14.85	Unknown	40.1	Threshold	
	2	Open	5:46:23	26.5	551.5	26.07	88	11.9	Not detected	
	3	Open	5:46:00	5.2	21.2	1.00	641		Not detected	
	6	Open	5:46:00	5.2	21.2	1.00	7		Undetectable	
	7	Open	5:46:25	20.0	314.2	14.85	355	33.1	Threshold	
	8	Beneath canopy	5:51:52	20.0	314.2	14.85	295	35.6	Threshold	
	9	Beneath canopy	5:51:52	30.0	706.9	33.41	235	23.6	Threshold	
	10	Beneath canopy	5:46:00	5.2	21.2	1.00	6		Undetectable	
	11	Beneath canopy	5:46:24	20.0	314.2	14.85	Unknown	34.8	Threshold	
	12	Beneath canopy	5:46:23	30.0	706.9	33.41	157	18.1	Background	
	13	Beneath canopy	5:46:00	5.2	21.2	1.00	Unknown		Unknown	
	4000	1	Open	5:25:06	20.0	314.2	8.17	Unknown	28.2	Threshold
		2	Open	5:25:07	26.5	551.5	14.35	165	14.6	Background
3		Open	5:25:00	5.2	21.2	0.55	645		Not detected	
6		Open	5:25:00	5.2	21.2	0.55	8		Undetectable	
7		Open	5:25:09	20.0	314.2	8.17	348	24.1	Threshold	
8		Beneath canopy	5:25:09	20.0	314.2	8.17	316	25.5	Threshold	
9		Beneath canopy	5:25:08	30.0	706.9	18.39	224	13.7	Background	
10		Beneath canopy	5:25:00	5.2	21.2	0.55	259		Not detected	
11		Beneath canopy	5:25:07	20.0	314.2	8.17	Unknown	27.1	Threshold	
12		Beneath canopy	5:25:07	30.0	706.9	18.39	143	14.3	Background	
13		Beneath canopy	5:25:00	5.2	21.2	0.55	Unknown		Unknown	
6000		1	Open	5:03:13	20.0	314.2	3.71	Unknown	13.0	Threshold
		2	Open	5:03:13	26.5	551.5	6.52	176	8.6	Background
	3	Open	5:03:00	5.2	21.2	0.25	322		Not detected	
	6	Open	5:03:00	5.2	21.2	0.25	603		Not detected	
	7	Open	5:03:15	20.0	314.2	3.71	325	11.9	Background	
	8	Beneath canopy	5:03:15	20.0	314.2	3.71	303	13.1	Background	
	9	Beneath canopy	5:03:15	30.0	706.9	8.35	172	6.1	Not detected	
	10	Beneath canopy	5:03:00	5.2	21.2	0.25	176		Not detected	
	11	Beneath canopy	5:03:13	20.0	314.2	3.71	Unknown	12.5	Background	
	12	Beneath canopy	5:03:13	30.0	706.9	8.35	140	6.1	Not detected	
	13	Beneath canopy	5:03:00	5.2	21.2	0.25	Unknown		Unknown	

^a Target number 4 failed completely, and target 5 was a non-target.

rough terrain (70% slope) associated with the coal seam precluded accurate measurements, but it was approximately 30 × 70 m on the ground with highly variable actual surface temperatures of 55 to 250°C.

Of the confirmed detectable artificial targets, AWIS detected 75, 78, and 50% of the confirmed detectable artificial targets at altitudes of 3000, 4000, and 6000 feet, respectively. BD FLIR detected 60, 30, and 11% of the targets at altitudes of 2000, 4000, and 6000 feet, respectively. The interpretation of BD FLIR information also resulted in the

identification of one false target at 4000 feet and another at 6000 feet, whereas no false targets were identified by AWIS.

Trial results suggest that hotspot detection capabilities decline rapidly with altitude (Tables 2 and 3). Many of the detection failures can be attributed to AWIS's inability to detect the smallest (5.2 cm in diameter) yet hottest (greater than 600°C) targets at all test altitudes. The presence or absence of a forest canopy did not appear to greatly influence detectability during these trials (Table 2), although targets were intention-

Table 3. Size and temperature of each target as reported at the time of imaging by BD FLIR

Mission altitude (feet)	Target identifier ^a	Target exposure	Time of sample	Target diameter (cm)	Target area (cm ²)	Target to pixel area ratio (%)	Actual target temperature (C)	Detection status
2000	1	Open	7:32:31	20.0	314.2	4.24	459	Background
	2	Open	7:32:31	26.5	551.5	7.44	124	Not detected
	3	Open	7:32:31	5.2	21.2	0.29	Unknown	Unknown
	4	Open	7:32:31	30.0	706.9	9.54	241	Background
	6	Open	7:32:31	5.2	21.2	0.29	5.6	Undetected
	7	Open	7:32:31	20.0	314.2	4.24	238	Background
	8	Beneath canopy	7:32:31	20.0	314.2	4.24	424	Background
	9	Beneath canopy	7:32:31	30.0	706.9	9.54	87	Not detected
	10	Beneath canopy	7:32:31	5.2	21.2	0.29	226	Not detected
	11	Beneath canopy	7:32:31	20.0	314.2	4.24	361	Background
	12	Beneath canopy	7:32:31	30.0	706.9	9.54	196	Background
	13	Beneath canopy	7:32:31	5.2	21.2	0.29	667	Not detected
	4000	1	Open	7:56:03	20.0	314.2	1.06	452
2		Open	7:56:03	26.5	551.5	1.86	125	Not detected
3		Open	7:56:03	5.2	21.2	0.07	Unknown	Unknown
4		Open	7:56:03	30.0	706.9	2.38	228	Not detected
6		Open	7:56:03	5.2	21.2	0.07	7.5	Undetected
7		Open	7:56:03	20.0	314.2	1.06	255	Not detected
8		Beneath canopy	7:56:03	20.0	314.2	1.06	422	Background
9		Beneath canopy	7:56:03	30.0	706.9	2.38	87	Not detected
10		Beneath canopy	7:56:03	5.2	21.2	0.07	238	Not detected
11		Beneath canopy	7:56:03	20.0	314.2	1.06	388	Not detected
12		Beneath canopy	7:56:03	30.0	706.9	2.38	190	Background
13		Beneath canopy	7:56:03	5.2	21.2	0.07	618	Not detected
6000		1	Open	8:08:39	20.0	314.2	0.47	444
	2	Open	8:08:39	26.5	551.5	0.83	127	Not detected
	3	Open	8:08:39	5.2	21.2	0.03	Unknown	Unknown
	4	Open	8:08:39	30.0	706.9	1.06	223	Not detected
	6	Open	8:08:39	5.2	21.2	0.03	8.7	Undetectable
	7	Open	8:08:39	20.0	314.2	0.47	256	Not detected
	8	Beneath canopy	8:08:39	20.0	314.2	0.47	421	Not detected
	9	Beneath canopy	8:08:39	30.0	706.9	1.06	89	Not detected
	10	Beneath canopy	8:08:39	5.2	21.2	0.03	254	Not detected
	11	Beneath canopy	8:08:39	20.0	314.2	0.47	389	Not detected
	12	Beneath canopy	8:08:39	30.0	706.9	1.06	188	Not detected
	13	Beneath canopy	8:08:39	5.2	21.2	0.03	4.6	Undetectable

^a Target 5 was a non-target.

ally placed within the forest so they would not be directly obscured planimetrically.

Imaged temperatures reported by AWIS, while perhaps applicable for relative categorization, do not accurately reflect actual temperatures. This may be of concern if imagery is to support documentation during litigation. The low imaged temperatures result because only a small portion of the image element (pixel) receives energy from the target surface. The energy emitted from

the target surface is diffused over the whole image or over multiple pixels due to distance that also attenuates the signal. This diffusion is apparent in the imagery and many pixels (up to about 20) are affected by the target's energy, although in theory only a maximum of four pixels should be partially affected. More work is required to establish methods to minimize this diffusion, and develop accurate relationships between imaged and actual temperatures.

Models for probability of hotspot detection

Probability of detection was modelled for AWIS and BD FLIR using logistic regression. Explanatory variables included hotspot temperature (Htemp, °C) and the size of the target hotspot as a proportion of a single image pixel on the ground.

The target-to-pixel area (TPA) defines the proportion of a single image pixel that is occupied by a given hotspot, calculated as:

$$TPA = Hsize/PA \cdot 100$$

where:

Hsize = size of the hotspot (cm²)

PA = dimension of a single image pixel on the ground (cm²)

The area (PA, in cm²) of a single image pixel on the ground is defined by altitude of the aircraft and the specifications of the image sensor (Matthews 1997):

$$PA = (\text{TAN}(\text{FOV}_x/2 \cdot \pi/180) \cdot \text{Altitude} \cdot 0.3048 / P_x) \cdot (\text{TAN}(\text{FOV}_y/2 \cdot \pi/180) \cdot \text{Altitude} \cdot 0.3048 / P_y) \cdot 10000$$

where:

FOV_x = sensor field of view in degrees in x direction

FOV_y = sensor field of view in degrees in y direction

P_x = number of image pixels in x direction

P_y = number of image pixels in y direction

Altitude = altitude of aircraft in feet above ground level

TAN = tangent of angle where angle is given in radians

Separate models were fitted to the data given in Tables 2 and 3 to describe the probability of detecting a hotspot using AWIS and BD FLIR:

$$\text{DetectionProb}_{\text{AWIS}} = 1/(1+\text{EXP}(-(-14.295+0.041 \cdot \text{LN}(\text{TPA}) \cdot \text{Htemp}))) \cdot 100$$

$$\text{McFadden's Rho-Squared} = 0.812$$

$$\text{DetectionProb}_{\text{BD FLIR}} = 1/(1+\text{EXP}(-(-6.616+0.016 \cdot \text{Htemp}+2.364 \cdot \text{LN}(\text{TPA})))) \cdot 100$$

$$\text{McFadden's Rho-Squared} = 0.498$$

where:

EXP = e to the power of a given number

LN = natural logarithm of a number

Slightly different statistical models were likely required because AWIS involved more image processing and interpretation than those normally applied during BD FLIR operations. Both of these models have been implemented to produce simple tables that can be used to derive detection probabilities for a variety of scenarios (Appendix I).

Both datasets were also merged to develop a generic probability of hotspot detection model. The model could be used to assess the potential detection performance of any sensor at a given altitude, when a trained thermographer is available to interpret the imagery.

$$\text{DetectionProb} = 1/(1+\text{EXP}(-(-1.486+0.007 \cdot \text{LN}(\text{TPA}) \cdot \text{Htemp}))) \cdot 100$$

$$\text{McFadden's Rho-Squared} = 0.476$$

By varying sensor specifications and flight altitudes, this theoretical model can be used to evaluate a variety of sensors in a variety of aircraft, including sensors used in helicopters.

Models for cost effectiveness

A simple model has been developed to allow fire managers to compare the costs of various infrared remote sensing systems and workloads, in the form of flight hours. The model was not designed to produce definitive mission costs, but rather can be used to compare the relative costs and mission flight times for various sensors and aircraft platforms.

Users are required to define the detection probability objectives for the mission, e.g., to detect 90 out of 100 smouldering hotspots (300°C) that are 25 cm² in size or greater.

The probability of detection models developed in this study are then applied, using the appropriate sensor specifications (FOV_x, FOV_y, P_x, and P_y), to determine the highest flight altitude that will meet the detection probability objectives for the mission.

In Table 4, sample user inputs are given for several infrared sensors—the AWIS and FLIR, as well as the AGA 750 handheld sensor mounted in a helicopter. Preliminary model outputs are calculated to determine the optimum mission altitude and area-scanning rate (area/h) for each sensor/platform configuration.

Although formal field trials have not been carried out to evaluate the performance of rotary wing and handheld scanning operations, a theoretical costing scenario has been included here to illustrate how the models can be expanded to consider how various aircraft and infrared scanner specifications might impact scanning costs. The scene width of rotary wing and handheld scanner operations may be expanded greatly, possibly up to double, by the operator panning the scanner. However, this scenario uses a conservative single scene width because the exact impact of panning on effective scene width is unknown.

The model calculates the time required by a specific aircraft to scan a given area, based on the optimum altitude and the operational scanning speed of the aircraft. Operational aircraft scanning speeds (km/h), aircraft costs (\$/h), and ferry times are entered by the user and applied to derive a total mission flight time (h) and cost for a fire of a given area or perimeter length. Sample model outputs are given in Table 5.

Model users must check the scene width to ensure it meets a minimum scan width of 100 m. This width would be required to support mop-up operations. In this case, the flight times and costs for the perimeter scanning missions must be tripled since the scene width is less than the minimum 100 m required. This can only be achieved by three passes at optimum altitude.

Users should also be aware that minimum flight altitudes for BD aircraft are 75 feet under VFR conditions during the day, and 500 or 1000 feet under VFR or IFR conditions over flat ground at night. AWIS missions are also limited to 1000 feet under IFR conditions over flat ground at night, but operational missions are rarely undertaken below 3000 feet above ground level. In both cases, nighttime

Table 4. Sample user inputs used to calculate optimum mission altitude, width, and area-scanning rate

	Aircraft and infrared sensor specifications		
	AWIS ^a	BD FLIR 2000	Rotary wing & AGA 750
Inputs			
FOV _x	n.a.	28	20
FOV _y	n.a.	15	20
Pixels across (x)	n.a.	354	106
Pixels down (y)	n.a.	186	106
Hotspot size (cm ²)	25	25	25
Probability of detection	90	90	90
Hotspot temperature (°C)	300	300	300
Aircraft scanning (\$/h)	1 746	676	1 065
Scanning speed (km/h)	278	222	40
Ferry time (h)	1.5	1.5	0
Calculated values			
Altitude (feet above ground level)	3 349	995	410
Scene width (m)	360	151	44
Area/h (m ² /h)	10 007	3 357	176

^a AWIS sensor specifications are proprietary information and hence are not included here.

Table 5. Total mission flight times and costs for fire of given area or perimeter length when aircraft scanning speeds, ferry times, and aircraft costs are input

Fire area (ha)	Equivalent fire perimeter (km)	Fire mission flight time (h) ^a			Flight costs (\$)		
		AWIS	BD FLIR	Rotary wing & AGA 750	AWIS	BD FLIR	Rotary wing & AGA 750
25	2.5	1.50	1.51	0.14	2 623	1 019	151
30	3.0	1.50	1.51	0.17	2 624	1 020	181
35	3.5	1.50	1.51	0.20	2 625	1 021	211
40	4.0	1.50	1.51	0.23	2 626	1 022	242
45	4.5	1.50	1.51	0.26	2 627	1 023	272
50	5.0	1.50	1.51	0.28	2 628	1 024	302
100	10.0	1.51	1.53	0.57	2 636	1 034	604
150	15.0	1.51	1.54	0.85	2 645	1 044	906
200	20.0	1.52	1.56	1.13	2 654	1 054	1 208
250	25.0	1.52	1.57	1.42	2 663	1 064	1 510
300	30.0	1.53	1.59	1.70	2 671	1 074	1 812
350	35.0	1.53	1.60	1.99	2 680	1 084	2 115
400	40.0	1.54	1.62	2.27	2 689	1 095	2 417
450	45.0	1.54	1.63	2.55	2 698	1 105	2 719
500	50.0	1.55	1.65	2.84	2 706	1 115	3 021
750	75.0	1.57	1.72	4.25	2 750	1 165	4 531
1 000	100.0	1.60	1.80	5.67	2 793	1 215	6 041
2 000	200.0	1.70	2.10	11.35	2 968	1 417	12 083
3 000	300.0	1.80	2.39	17.02	3 142	1 618	18 124
4 000	400.0	1.90	2.69	22.69	3 317	1 819	24 166
5 000	500.0	2.00	2.99	28.36	3 491	2 021	30 207
10 000	1 000.0	2.50	4.48	56.73	4 364	3 028	60 415
20 000	2 000.0	3.50	7.46	113.45	6 108	5 041	120 829
40 000	4 000.0	5.50	13.41	226.91	9 598	9 068	241 658
50 000	5 000.0	6.50	16.39	283.64	11 342	11 082	302 073
60 000	6 000.0	7.50	19.37	340.36	13 087	13 095	362 488
80 000	8 000.0	9.49	25.33	453.82	16 577	17 122	483 317
100 000	10 000.0	11.49	31.29	567.27	20 066	21 149	604 146
200 000	20 000.0	21.49	61.07	1 134.55	37 513	41 284	1 208 292

^a Flight times in **bold** indicate that it is unlikely that the mission will be completed in a single morning.

missions would usually be carried out under VFR conditions.

Several assumptions have been made in the development of this model:

- The maximum feasible morning mission duration is 1 h for VFR aircraft.
- The maximum feasible morning mission duration is 4 h for IFR aircraft.
- Flight times and costs are based on fire area or perimeter scans assuming a perimeter scan width of 100 m.
- The rotary wing and handheld scanner scenario does not reflect the fact that the scene width can be expanded if the operator pans the scanner.

- Costs are based on aircraft costs only (fuel in).
- There is zero turnaround time at the edge of flight paths.

The results suggest that for fires less than 150 ha or when perimeter scanning in support of mop-up operations is less than about 15 km, rotary wing missions with an AGA 750 are more cost effective than AWIS or BD FLIR. The cost of BD FLIR operations is less than half that of AWIS until fires exceed about 2000 ha or perimeter scanning exceeds 200 km.

Conclusions

Field trials were used to develop methods and models to assess and quantify the detection capabilities of infrared systems such as AWIS and BD FLIR. The trials showed that AWIS detected 75, 78, and 50% of the detectable artificial targets at altitudes of 3000, 4000, and 6000 feet, respectively. BD FLIR detected 60, 30, and 11% of the targets at altitudes of 2000, 4000, and 6000 feet, respectively. The interpretation of BD FLIR information also resulted in the identification of one false target at 4000 feet and another at 6000 feet, whereas no false targets were identified by AWIS.

Field trial results suggest that there are limitations for the application of AWIS and BD FLIR to support mop-up operations by way of the detection of subtle hotspots. Such detection limitations may or may not be critical depending on user expectations. Subsequent field trials could include target-to-pixel area ratios of about 5–10%, which would expand the range of conditions evaluated. Nonetheless, the data collected have been applied to establish detection threshold models, which can be used to indicate the temperature and size of minimum detectable hotspots for a given altitude. These models are useful for mission and flight planning during wildfire operation.

Trial results suggest that hotspot detection capabilities decline rapidly with altitude, which is expected given the decrease in target-to-pixel area ratio. Many of the detection failures can be attributed to the inability of AWIS to detect the smallest (5.2 cm in diameter) yet hottest targets (greater than 600°C) at all test altitudes. The presence or absence of a forest canopy did not appear to greatly influence the success of detection during these trials, although targets were intentionally placed within the forest so they would not be obscured planimetrically.

The probability of detecting a hotspot using infrared remote sensing techniques depends on the size and temperature of the

hotspot, the specifications of the infrared sensor, and the altitude at which scanning is conducted. The probability of detection models developed can be applied to set infrared remote sensing mission objectives, and to help fire managers assess the cost effectiveness of alternative detection technologies.

Results of the costing models developed suggest that rotary wing missions with an AGA 750 are more cost effective than AWIS or BD FLIR for fires less than 150 ha or when perimeter scanning in support of mop-up operations is less than about 15 km. BD FLIR operations cost less than half that of AWIS until fires exceed about 2000 ha or perimeter scanning exceeds 200 km. Thereafter, the costs for AWIS and BD FLIR missions become more similar, although the products and information delivered to fireline staff using these services may differ greatly.

References

- Aldrich, R. 1979. Remote sensing of wildland resources: a state-of-the-art review. U.S. Department of Agriculture, Forest Service, Rocky Mountain Forest and Range Experiment Station, Fort Collins, Colo. General Technical Report RM-71.
- Billings, P. 1986. Operational aspects of the infra-red line scanner. Department of Conservation and Environment, Victoria, Australia. Fire Protection Branch Research Report No. 26.
- Campbell, D.; Born, W.; Beck, J.; Bereska, B.; Frederick, K.; Hua, S. 2002. The airborne wildfire intelligence system: a decision support tool for wildland fire managers in Alberta. Society of Photo-Optical Instrumentation Engineers (SPIE). Paper number 4710-20.
- Matthews, A. 1997. FIRESCAN: a technique for airborne infrared mapping of wildfires. Ph.D. thesis prepared for the Department of Earth Sciences, Monash University, Australia.

Niederleitner, J. 1976. Detecting holdover fires with the AGA Thermovision 750 infrared scanner. Canadian Forest Service, Northern Forest Research Centre, Edmonton, Alta. Information Report Nor-X-151.

Ogilvie, C.J.; Young, R.W. 1989. Daedalus line scanner trials in Alberta, 1985 and 1986. Forestry Canada, Northern Forestry Centre, Edmonton, Alta. Information Report NOR-X-298.

Woodard, P.M.; Adamowicz, W.L.; Bolster, O.J. 1993. An economic evaluation of forward looking infrared (FLIR) technology to enhance aerial suppression of forest fires in Alberta. Forestry Canada, Northern Forestry Centre, Edmonton, Alta. Canada-Alberta Partnership Agreement in Forestry Report 105.

Acknowledgements

Thanks to those who assisted with field trial work including Ray Ault, Gary Dakin, Greg Baxter, and Rex Hsieh of FERIC; Chuck Ogilvie, formerly of the Canadian Forest Service; Weldwood of Canada Limited, Hinton Division; Mark Ackerman and Shirley Niven of the University of Alberta; Dennis Driscoll and Wally Born of Alberta Sustainable Resource Development; and staff at the Edson Wildfire Management Area.

Appendix I

Tables to predict probability of hotspot detection ^a

Probability of hotspot detection using AWIS

Altitude ^b (ft.)	Hotspot size (cm ²)	Hotspot temperature (°C)											
		50	100	150	200	250	300	350	400	450	500	550	600
500	10	<i>0</i>	95	100	100	100	100	100	100	100	100	100	100
	25	<i>2</i>	100	100	100	100	100	100	100	100	100	100	100
	50	<i>9</i>	100	100	100	100	100	100	100	100	100	100	100
	100	<i>29</i>	100	100	100	100	100	100	100	100	100	100	100
	200	<i>63</i>	100	100	100	100	100	100	100	100	100	100	100
	300	79	100	100	100	100	100	100	100	100	100	100	100
	400	87	100	100	100	100	100	100	100	100	100	100	100
	500	92	100	100	100	100	100	100	100	100	100	100	100
	1 000	98	100	100	100	100	100	100	100	100	100	100	100
	2 000	99	100	100	100	100	100	100	100	100	100	100	100
	3 000	100	100	100	100	100	100	100	100	100	100	100	100
	4 000	100	100	100	100	100	100	100	100	100	100	100	100
	5 000	100	100	100	100	100	100	100	100	100	100	100	100
10 000	100	100	100	100	100	100	100	100	100	100	100	100	
1 000	10	<i>0</i>	<i>7</i>	96	100	100	100	100	100	100	100	100	100
	25	<i>0</i>	75	100	100	100	100	100	100	100	100	100	100
	50	<i>1</i>	98	100	100	100	100	100	100	100	100	100	100
	100	<i>2</i>	100	100	100	100	100	100	100	100	100	100	100
	200	<i>9</i>	100	100	100	100	100	100	100	100	100	100	100
	300	<i>18</i>	100	100	100	100	100	100	100	100	100	100	100
	400	<i>29</i>	100	100	100	100	100	100	100	100	100	100	100
	500	<i>39</i>	100	100	100	100	100	100	100	100	100	100	100
	1 000	73	100	100	100	100	100	100	100	100	100	100	100
	2 000	92	100	100	100	100	100	100	100	100	100	100	100
	3 000	96	100	100	100	100	100	100	100	100	100	100	100
	4 000	98	100	100	100	100	100	100	100	100	100	100	100
	5 000	99	100	100	100	100	100	100	100	100	100	100	100
10 000	100	100	100	100	100	100	100	100	100	100	100	100	
1 500	10	<i>0</i>	<i>0</i>	<i>14</i>	91	100	100	100	100	100	100	100	100
	25	<i>0</i>	<i>10</i>	98	100	100	100	100	100	100	100	100	100
	50	<i>0</i>	<i>65</i>	100	100	100	100	100	100	100	100	100	100
	100	<i>0</i>	97	100	100	100	100	100	100	100	100	100	100
	200	<i>2</i>	100	100	100	100	100	100	100	100	100	100	100
	300	<i>4</i>	100	100	100	100	100	100	100	100	100	100	100
	400	<i>7</i>	100	100	100	100	100	100	100	100	100	100	100
	500	<i>11</i>	100	100	100	100	100	100	100	100	100	100	100
	1 000	<i>33</i>	100	100	100	100	100	100	100	100	100	100	100
	2 000	<i>67</i>	100	100	100	100	100	100	100	100	100	100	100
	3 000	83	100	100	100	100	100	100	100	100	100	100	100
	4 000	90	100	100	100	100	100	100	100	100	100	100	100
	5 000	93	100	100	100	100	100	100	100	100	100	100	100
10 000	98	100	100	100	100	100	100	100	100	100	100	100	

^a Numbers indicate that the probability of detection is greater than 95%, except those that are *italicized* indicate 0–70% probability, and those that are **bolded** indicate 70–95% probability.

^b Above ground level.

Appendix I

Tables to predict probability of hotspot detection (continued) ^a

		Probability of hotspot detection using AWIS											
Altitude ^b (ft.)	Hotspot size (cm ²)	Hotspot temperature (°C)											
		50	100	150	200	250	300	350	400	450	500	550	600
2 000	10	33	60	82	93	98	99	100	100	100	100	100	100
	25	50	86	97	100	100	100	100	100	100	100	100	100
	50	63	94	99	100	100	100	100	100	100	100	100	100
	100	74	98	100	100	100	100	100	100	100	100	100	100
	200	83	99	100	100	100	100	100	100	100	100	100	100
	300	87	100	100	100	100	100	100	100	100	100	100	100
	400	89	100	100	100	100	100	100	100	100	100	100	100
	500	90	100	100	100	100	100	100	100	100	100	100	100
	1 000	94	100	100	100	100	100	100	100	100	100	100	100
	2 000	96	100	100	100	100	100	100	100	100	100	100	100
	3 000	97	100	100	100	100	100	100	100	100	100	100	100
	4 000	98	100	100	100	100	100	100	100	100	100	100	100
	5 000	98	100	100	100	100	100	100	100	100	100	100	100
	10 000	99	100	100	100	100	100	100	100	100	100	100	100
4 000	10	0	0	0	0	0	0	0	0	0	0	0	0
	25	0	0	0	0	1	10	46	87	98	100	100	100
	50	0	0	2	37	95	100	100	100	100	100	100	100
	100	0	1	57	99	100	100	100	100	100	100	100	100
	200	0	15	99	100	100	100	100	100	100	100	100	100
	300	0	48	100	100	100	100	100	100	100	100	100	100
	400	0	75	100	100	100	100	100	100	100	100	100	100
	500	0	88	100	100	100	100	100	100	100	100	100	100
	1 000	1	99	100	100	100	100	100	100	100	100	100	100
	2 000	4	100	100	100	100	100	100	100	100	100	100	100
	3 000	8	100	100	100	100	100	100	100	100	100	100	100
	4 000	13	100	100	100	100	100	100	100	100	100	100	100
	5 000	20	100	100	100	100	100	100	100	100	100	100	100
	10 000	50	100	100	100	100	100	100	100	100	100	100	100
6 000	10	0	0	0	0	0	0	0	0	0	0	0	0
	25	0	0	0	0	0	0	0	0	0	0	0	0
	50	0	0	0	0	0	3	14	48	85	97	99	100
	100	0	0	1	18	85	99	100	100	100	100	100	100
	200	0	1	39	99	100	100	100	100	100	100	100	100
	300	0	3	89	100	100	100	100	100	100	100	100	100
	400	0	10	98	100	100	100	100	100	100	100	100	100
	500	0	21	99	100	100	100	100	100	100	100	100	100
	1 000	0	82	100	100	100	100	100	100	100	100	100	100
	2 000	1	99	100	100	100	100	100	100	100	100	100	100
	3 000	2	100	100	100	100	100	100	100	100	100	100	100
	4 000	3	100	100	100	100	100	100	100	100	100	100	100
	5 000	4	100	100	100	100	100	100	100	100	100	100	100
	10 000	16	100	100	100	100	100	100	100	100	100	100	100

^a Numbers indicate that the probability of detection is greater than 95%, except those that are *italicized* indicate 0–70% probability, and those that are **bolded** indicate 70–95% probability.

^b Above ground level.

Appendix I

Tables to predict probability of hotspot detection (continued) ^a

Probability of hotspot detection using FLIR 2000

Altitude ^b (ft.)	Hotspot size (cm ²)	Hotspot temperature (°C)											
		50	100	150	200	250	300	350	400	450	500	550	600
500	10	32	52	71	84	92	96	98	99	100	100	100	100
	25	81	90	95	98	99	100	100	100	100	100	100	100
	50	96	98	99	100	100	100	100	100	100	100	100	100
	100	99	100	100	100	100	100	100	100	100	100	100	100
	200	100	100	100	100	100	100	100	100	100	100	100	100
	300	100	100	100	100	100	100	100	100	100	100	100	100
	400	100	100	100	100	100	100	100	100	100	100	100	100
	500	100	100	100	100	100	100	100	100	100	100	100	100
	1 000	100	100	100	100	100	100	100	100	100	100	100	100
	2 000	100	100	100	100	100	100	100	100	100	100	100	100
	3 000	100	100	100	100	100	100	100	100	100	100	100	100
	4 000	100	100	100	100	100	100	100	100	100	100	100	100
	5 000	100	100	100	100	100	100	100	100	100	100	100	100
	10 000	100	100	100	100	100	100	100	100	100	100	100	100
1 000	10	2	4	8	17	31	50	69	83	92	96	98	99
	25	14	26	44	64	80	90	95	98	99	100	100	100
	50	45	65	80	90	95	98	99	100	100	100	100	100
	100	81	90	95	98	99	100	100	100	100	100	100	100
	200	96	98	99	100	100	100	100	100	100	100	100	100
	300	98	99	100	100	100	100	100	100	100	100	100	100
	400	99	100	100	100	100	100	100	100	100	100	100	100
	500	99	100	100	100	100	100	100	100	100	100	100	100
	1 000	100	100	100	100	100	100	100	100	100	100	100	100
	2 000	100	100	100	100	100	100	100	100	100	100	100	100
	3 000	100	100	100	100	100	100	100	100	100	100	100	100
	4 000	100	100	100	100	100	100	100	100	100	100	100	100
	5 000	100	100	100	100	100	100	100	100	100	100	100	100
	10 000	100	100	100	100	100	100	100	100	100	100	100	100
1 500	10	0	1	1	3	6	13	25	42	62	78	89	95
	25	2	5	10	21	37	56	74	86	93	97	99	99
	50	11	21	38	57	75	87	94	97	99	99	100	100
	100	38	58	76	87	94	97	99	99	100	100	100	100
	200	76	88	94	97	99	99	100	100	100	100	100	100
	300	89	95	98	99	100	100	100	100	100	100	100	100
	400	94	97	99	99	100	100	100	100	100	100	100	100
	500	97	98	99	100	100	100	100	100	100	100	100	100
	1 000	99	100	100	100	100	100	100	100	100	100	100	100
	2 000	100	100	100	100	100	100	100	100	100	100	100	100
	3 000	100	100	100	100	100	100	100	100	100	100	100	100
	4 000	100	100	100	100	100	100	100	100	100	100	100	100
	5 000	100	100	100	100	100	100	100	100	100	100	100	100
	10 000	100	100	100	100	100	100	100	100	100	100	100	100

^a Numbers indicate that the probability of detection is greater than 95%, except those that are *italicized* indicate 0–70% probability, and those that are **bolded** indicate 70–95% probability.

^b Above ground level.

Appendix I

Tables to predict probability of hotspot detection (continued) ^a

		Probability of hotspot detection using FLIR 2000											
Altitude ^b (ft.)	Hotspot size (cm ²)	Hotspot temperature (°C)											
		50	100	150	200	250	300	350	400	450	500	550	600
2 000	10	<i>0</i>	<i>0</i>	<i>0</i>	<i>1</i>	<i>2</i>	<i>4</i>	<i>8</i>	<i>16</i>	<i>29</i>	<i>48</i>	<i>67</i>	82
	25	<i>1</i>	<i>1</i>	<i>3</i>	<i>6</i>	<i>13</i>	<i>25</i>	<i>42</i>	<i>62</i>	78	89	95	98
	50	<i>3</i>	<i>6</i>	<i>13</i>	<i>26</i>	<i>43</i>	<i>63</i>	79	89	95	98	99	100
	100	<i>14</i>	<i>26</i>	<i>44</i>	<i>64</i>	80	90	95	98	99	100	100	100
	200	<i>45</i>	<i>65</i>	80	90	95	98	99	100	100	100	100	100
	300	<i>68</i>	83	91	96	98	99	100	100	100	100	100	100
	400	81	90	95	98	99	100	100	100	100	100	100	100
	500	88	94	97	99	99	100	100	100	100	100	100	100
	1 000	97	99	99	100	100	100	100	100	100	100	100	100
	2 000	99	100	100	100	100	100	100	100	100	100	100	100
	3 000	100	100	100	100	100	100	100	100	100	100	100	100
	4 000	100	100	100	100	100	100	100	100	100	100	100	100
	5 000	100	100	100	100	100	100	100	100	100	100	100	100
	10 000	100	100	100	100	100	100	100	100	100	100	100	100
4 000	10	<i>0</i>	<i>0</i>	<i>0</i>	<i>0</i>	<i>0</i>	<i>0</i>	<i>0</i>	<i>1</i>	<i>2</i>	<i>3</i>	<i>7</i>	<i>15</i>
	25	<i>0</i>	<i>0</i>	<i>0</i>	<i>0</i>	<i>1</i>	<i>1</i>	<i>3</i>	<i>6</i>	<i>12</i>	<i>23</i>	<i>41</i>	<i>60</i>
	50	<i>0</i>	<i>0</i>	<i>1</i>	<i>1</i>	<i>3</i>	<i>6</i>	<i>12</i>	<i>24</i>	<i>41</i>	<i>61</i>	78	89
	100	<i>1</i>	<i>1</i>	<i>3</i>	<i>6</i>	<i>13</i>	<i>25</i>	<i>42</i>	<i>62</i>	78	89	95	98
	200	<i>3</i>	<i>6</i>	<i>13</i>	<i>26</i>	<i>43</i>	<i>63</i>	79	89	95	98	99	100
	300	<i>8</i>	<i>15</i>	<i>29</i>	<i>47</i>	<i>67</i>	82	91	96	98	99	100	100
	400	<i>14</i>	<i>26</i>	<i>44</i>	<i>64</i>	80	90	95	98	99	100	100	100
	500	<i>21</i>	<i>38</i>	<i>57</i>	75	87	94	97	99	99	100	100	100
	1 000	<i>58</i>	76	87	94	97	99	99	100	100	100	100	100
	2 000	88	94	97	99	99	100	100	100	100	100	100	100
	3 000	95	98	99	100	100	100	100	100	100	100	100	100
	4 000	97	99	99	100	100	100	100	100	100	100	100	100
	5 000	98	99	100	100	100	100	100	100	100	100	100	100
	10 000	100	100	100	100	100	100	100	100	100	100	100	100
6 000	10	<i>0</i>	<i>0</i>	<i>0</i>	<i>0</i>	<i>0</i>	<i>0</i>	<i>0</i>	<i>0</i>	<i>0</i>	<i>1</i>	<i>1</i>	<i>2</i>
	25	<i>0</i>	<i>0</i>	<i>0</i>	<i>0</i>	<i>0</i>	<i>0</i>	<i>0</i>	<i>1</i>	<i>2</i>	<i>4</i>	<i>9</i>	<i>18</i>
	50	<i>0</i>	<i>0</i>	<i>0</i>	<i>0</i>	<i>0</i>	<i>1</i>	<i>2</i>	<i>4</i>	<i>9</i>	<i>19</i>	<i>34</i>	<i>53</i>
	100	<i>0</i>	<i>0</i>	<i>0</i>	<i>1</i>	<i>2</i>	<i>5</i>	<i>10</i>	<i>19</i>	<i>35</i>	<i>54</i>	73	86
	200	<i>0</i>	<i>1</i>	<i>2</i>	<i>5</i>	<i>10</i>	<i>20</i>	<i>36</i>	<i>55</i>	73	86	93	97
	300	<i>1</i>	<i>3</i>	<i>6</i>	<i>12</i>	<i>23</i>	<i>39</i>	<i>59</i>	76	88	94	97	99
	400	<i>2</i>	<i>5</i>	<i>10</i>	<i>21</i>	<i>37</i>	<i>56</i>	74	86	93	97	99	99
	500	<i>4</i>	<i>8</i>	<i>17</i>	<i>31</i>	<i>50</i>	<i>69</i>	83	92	96	98	99	100
	1 000	<i>17</i>	<i>31</i>	<i>50</i>	<i>69</i>	83	92	96	98	99	100	100	100
	2 000	<i>51</i>	70	84	92	96	98	99	100	100	100	100	100
	3 000	73	86	93	97	99	99	100	100	100	100	100	100
	4 000	85	92	96	98	99	100	100	100	100	100	100	100
	5 000	90	95	98	99	100	100	100	100	100	100	100	100
	10 000	98	99	100	100	100	100	100	100	100	100	100	100

^a Numbers indicate that the probability of detection is greater than 95%, except those that are *italicized* indicate 0–70% probability, and those that are **bolded** indicate 70–95% probability.

^b Above ground level.